IEEE Access
Multidisciplinary ⋮ Rapid Review ⋮ Open Access Journal

Received January 16, 2020, accepted March 6, 2020, date of publication March 10, 2020, date of current version March 19, 2020.

Digital Object Identifier 10.1109/ACCESS.2020.2979867

A Novel Dynamic Path Re-Planning Algorithm With Heading Constraints for Human Following Robots

HUI ZHANG[1], PEI WANG[1], YOUPAN ZHANG[1], BIN LI[2], AND YONGGUO ZHAO[3]

[1]School of Electrical Engineering and Automation, Qilu University of Technology (Shandong Academy of Sciences), Jinan 250353, China
[2]School of Mathematics and Statistics, Qilu University of Technology (Shandong Academy of Sciences), Jinan 250353, China
[3]Institute of Automation, Qilu University of Technology (Shandong Academy of Sciences), Jinan 250014, China

Corresponding author: Yongguo Zhao (sduzyg@163.com)

This work was supported in part by the Shandong Provincial Natural Science Foundation under Grant ZR2018LF011 and Grant ZR2018QF004, in part by the Shandong Province Key Research and Development Program under Grant 2019GGX104091 and Grant 2018GGX103054, in part by the Young Doctor Cooperation Foundation of the Qilu University of Technology (Shandong Academy of Sciences) under Grant 2018BSHZ006, and in part by the Development Plan of Young Innovation Team in Colleges and Universities of Shandong Province under Grant 2019KJN011.

ABSTRACT Paths will be re-planed timely according the change of obstacles and target position for Human Following Robots (HFRs) so that they can run safely and rapidly. Traditional path planning algorithms are generally focused on how to avoid obstacles or connect with the new target position effectively, however there are rarely studies on the elimination of robot heading fluctuation which is caused by path re-planning. Concerning this issue, we introduce a novel dynamic path re-planning algorithm AT* which is based on A* and walkable area thinning. When robots heading difference value between the current and the last moment which is derived from A* exceeds the threshold, AT* will search for path connection points by walkable area thinning, and then a new path going through optimal connection point and meeting heading constraints will be planned. Thinning algorithm is improved in order to make the passable skeleton can connect path origin and the end. Results from simulation experiments show that AT* algorithm keeps heading stability as a priority at path re-planning and the robot motion stability can be improved effectively.

INDEX TERMS Following robots, path planning, heading, thinning algorithm.

I. INTRODUCTION

With the development of modern robot technology, more and more robots are integrated into people's daily life and changing our lifestyle dramatically. More specifically, the capability to autonomously follow a person has been identified as an important functionality for many assistive and service robot systems. For example, the CaddyTrek can carry stuffs of user in golf course [1]. ROREASI follows stroke patients to provide them with continual assistance and guidance [2]. Budgee robot can follow behind a person and be used to carry the baskets when grocery shopping or your luggage during trips [3]. TMS Ariamatic 240 sweeper follows along the operator at a precise distance behind, this allows the operator to engage with the sole task of picking up debris with the wander hose without worrying about continuously moving the sweeper unit forward.

HFRs always work in dynamic environment where the interference of unexpected obstacles is inevitable, it needs robots to find a collision free trajectory from a designed start point to the target position. Existing path planning algorithms can be divided into global static planning stage and local dynamic planning stage [4]. Global path planning stage uses known environmental information to find a feasible path from the start point to a goal point by a search algorithm such as grid method [5], visibility graphs [6] or Voronoi graphs, etc. For local path planning stage, a path can be achieved by virtual force field [7], vector field histogram [8], fuzzy logic method [9] or artificial potential field method [10] based on dynamic environment information obtained from sensors.

A global map of the environment is occasionally not available in dynamic unknown environment [11], HFRs could only detect local sensory information of the environment to carry

The associate editor coordinating the review of this manuscript and approving it for publication was Eduardo Rosa-Molinar.

out the path planning task. Besides, the goal point is rarely static but changing all the time with the followed person movement, so there is an obvious difference between the classic path planning method which is only for a constant goal and the planning method which is suitable for human following. Path planning gets more challenging problems if the accurate localization of the mobile robot is not available under unstructured environment which leads to the path incremental update is infeasible. For these reasons, the path will have to be planned at current scene and then re-planned at the next scene, that is, there is a need to carry out local path planning frequently. However, most traditional path planning algorithms are generally focused on how to avoid obstacles or connect with the new target position, but work do not consider the elimination of robot heading fluctuation which is caused by path re-planning.

To address this, a novel dynamic path re-planning method based on A* algorithm and walkable area thinning (AT*) is proposed in this paper. When robots heading difference value between the current and last moment which is derived from the path planned by A* exceeds the threshold, AT* will search for connection points by walkable area thinning, and then a new path going through optimal connection point and meeting heading constraints will be re-planned. Thinning algorithm is improved in order to make the passable skeleton can connect path origin and the end. AT* can satisfy HFRs heading constraints in dynamic path re-planning with above modifications.

The organization of this paper is as follows: environment modeling method, A* algorithm as well as the existing problem are described in Section II. Detail of AT* method is described in Section III. Simulations are done to demonstrate the capability of AT* in Section IV, Conclusion and future work are drawn in Section V.

II. MAP BUILDING AND A* ALGORITHM

A. ENVIRONMENT DESCRIPTION

HFRs can only detect local sensory information of the environment. As the robot explores the environment, the map grows over time, and increasing computational resources are required, especially for large-scale environments [12], [13]. One of the most popular approaches to makes full use of the real-time local environmental information and solve local obstacle avoidance is dynamic window approach (DWA) [14].

In this paper, a grid map with regularly sized grid cells is used to represent the environment in DWA, and the projection of the followed person is selected as a temporary goal. Goal point and human location should be the same if the person is in the area of rolling window. On the other hand, if the human location is out of the rolling window, a goal projection will be selected out as a temporary goal. The selection method is that if the intersection point between the dynamic window and the line connecting the robot and the human is walkable, a route from the robot to the intersection will be planned; but if the intersection is un-walkable, the planner will search the dynamic window margin from the intersection to both sides until a walkable grid is found, and then the planner will search a path from the robot to this grid. The Fig. 1 shows the principle of temporary goal point selecting.

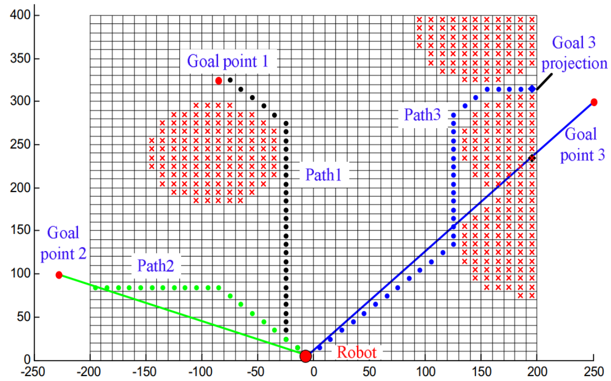

FIGURE 1. Goal generation.

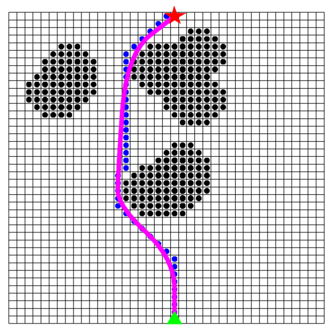

FIGURE 2. A* trajectory and smoothed path.

B. A* ALGORITHM AND THE EXISTING PROBLEM

Path planning is the key technology of robot navigation and obstacle avoidance [15]. There have been many path planning algorithms based on grid map, such as A* [16], D*, or focused D* (FD*) [17] algorithm. A* algorithm is an efficient heuristic path search algorithm for solving optimization problem of static path planning.

A* plans a path from an initial state $s_{star} \in S$ to a goal state $s_{goal} \in S$, where S is the set of states in some finite state space. This algorithm uses an evaluation function:

$$f(s) = g(s) + h(s) \tag{1}$$

where $f(s)$ is the value of the evaluation function for every node which will be searched possibly; $g(s)$ is the actual cost from start node to current node; $h(s)$ represents the assessment from current node to target node. The f-value of the goal is the length of the shortest path. A complete search process of A* algorithm is shown with blue points in Fig. 2. The green triangle represents the robot and red pentagon is the target. Obstacles are shown with black points.

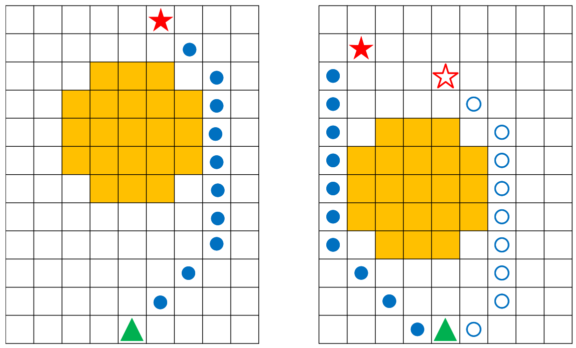

FIGURE 3. The current path and updated path.

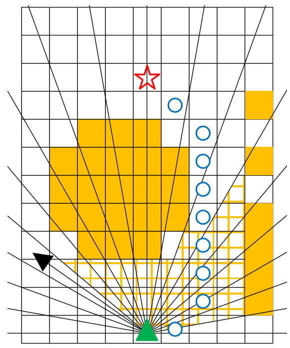

FIGURE 4. Example of an obstacle course by VFH.

The path output by searching over a regular grid is jagged. The large changes in heading in this path can induce undesirable steering commands [18], [19]. In order to make the route smoother, a quadratic B-splines curve expressed as (2) is used to generate a smooth path. the smoothed route is shown with magenta color.

$$P_{0,2}(t) = \frac{1}{2}\begin{bmatrix} 1 & t & t^2 \end{bmatrix}\begin{bmatrix} 1 & 1 & 0 \\ -2 & 2 & 0 \\ 1 & -2 & 1 \end{bmatrix}\begin{bmatrix} P_0 \\ P_1 \\ P_2 \end{bmatrix} \tag{2}$$

where P_0, P_1, and P_2 are the adjacent inflection points, and $P_{0,2}(t)$ is the smooth points connecting P_0, P_1, and P_2, $t \in [0, 1]$.

During the process of following, the goal point is rarely static but changing all the time, thus the current path will be invalid in the next moment. As shown in Fig. 3(a), the robot which is shown with green triangle walks along a blue path $\{R\}$ generated by A* to the red star target. Obstacles are shown with orange square blocks. Then the followed person will move to a new location and $\{R\}$ will be no longer connect to the new goal point. If the real time position information is not available, the existing path $\{R\}$ will not be updated to the new goal point incrementally, so a new path from the robot position to the current goal point is need to be re-planned. As shown in Fig. 3(b), blue hollow circles show the rest of $\{R\}$ and blue circles show the re-planned path. From this figure we can see that there is a large orientation difference between the last path and the updated which will lead to an obvious heading fluctuation. In fact, the local path planning needs to consider the robot motion constraints, otherwise, the planning path is not a feasible path [4].

In the current algorithms, vector field histogram (VFH) accomplish obstacle avoidance by heading adjusting [20]. It maps the active region C_a of the map grid C onto the primary polar histogram H^p. The active region is a circular window of diameters that moves with the robot. The content of each active cell(i, j) in the map grid is treated as an obstacle vector. The vector direction $\beta_{i,j}$ is determined by the direction from the active cell(i, j) to the robot center point (RCP),

$$\beta_{i,j} = \tan^{-1}\frac{y_i - y_0}{x_i - x_0} \tag{3}$$

(x_0, y_0) is the present coordinates of the RCP,
(x_j, y_j) is the Coordinates of active cell(i, j).
and the magnitude is given by

$$m_{i,j} = c_{i,j}(a - bd_{i,j}) \tag{4}$$

where a, b are positive constants, and $a - bd_{\max}^2 = 0$.

$$c_{i,j} = \begin{cases} 1 & \text{if cell}(i, j) \text{ is obstacle} \\ 0 & \text{if cell}(i, j) \text{ is free} \end{cases}$$

$d_{i,j}$ is the distance between active cell(i, j) and the RCP.
$m_{i,j}$ is proportional to $-d$.

Therefore, occupied cells produce large vector magnitudes when they are in the immediate vicinity of the robot, and smaller ones when they are further away. This way $m_{i,j} = 0$ for the farthest active cell and increases linearly for closer cells. H has an arbitrary angular resolution a such that $n = 360/\alpha$ is an integer(e.g., $\alpha = 10°$ and $n = 36$), so each sector k is

$$k = \mathrm{INT}(\beta_{i,j}/\alpha) \tag{5}$$

For each sector k, the polar obstacle density h_k is calculated by

$$h_k = \sum\nolimits_{i,j} m_{i,j} \tag{6}$$

Then the sector with lower cost and closer to the robot's pose will be selected as the forward direction, but the feasible path may be blocked when using this strategy, as shown in Fig. 4. If obstacles appear on the right side of the map, the direction to the left as shown by the arrow will be selected. VFH is a local obstacle avoidance strategy and apt to plunge into local minimum, there are some limitations on heading constraints using this algorithm.

III. AT* ALGORITHM

Focusing on the problem, a novel dynamic path re-planning method AT* which is based on A* algorithm and walkable area thinning is proposed. When robots heading difference value between the current and last moment which is derived from the path planned by A* exceeds a threshold, AT* will search for connection points by walkable area thinning, and

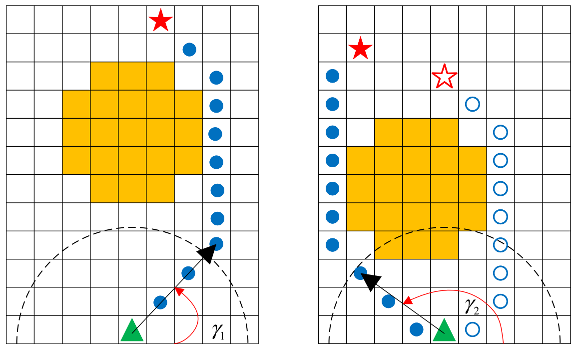

(a) Current direction angle (b) Updated direction angle

FIGURE 5. Desirable direction angle.

P9 (0)	P2 (1)	P3 (1)
P8 (1)	P1 (1)	P4 (0)
P7 (1)	P6 (1)	P5 (1)

FIGURE 6. Center cell P_1 and its8-neighbors.

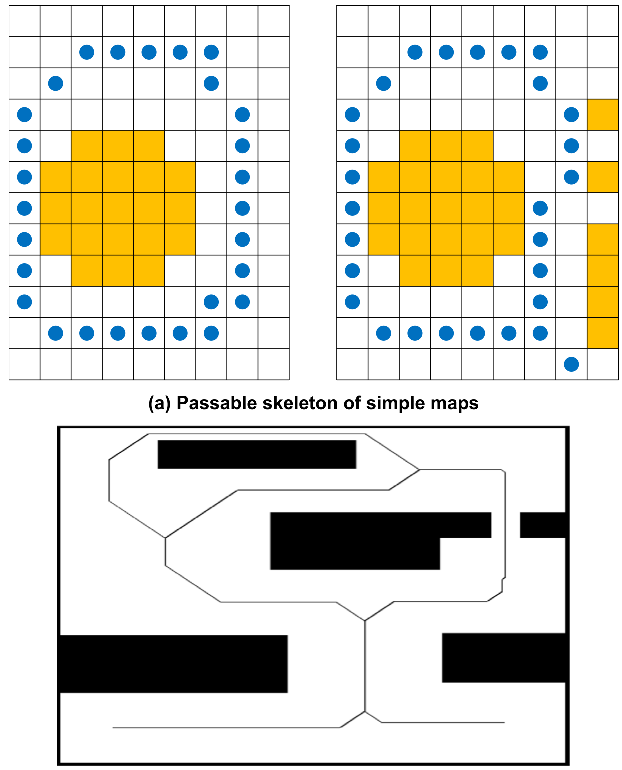

(a) Passable skeleton of simple maps

(b) Passable skeleton of complicated map

FIGURE 7. Thinning of different maps with Zhang-Suen algorithm.

then a new path going through optimal connection point will be re-planned.

For the path planned by A* as shown in Figure 3, the desirable direction angle is obtained by line-of-sight (LOS) method. The LOS vector starts at the robot and passes through a point (x_{los}, y_{los}), which is located on the path line at a lookahead distance $\Delta > 0$ ahead of the robot position (x_r, y_r) to the path, the direction angle is calculated by

$$\gamma = \tan^{-1} \frac{y_{los} - y_r}{x_{los} - x_r} \tag{7}$$

Setting Δ equals the length of four grids, Fig. 5 shows the current desirable direction angle γ_1 and the updated angle γ_2. If the absolute difference between γ_1 and γ_2 is less than threshold l, robots will walk along the updated path. Otherwise, the direction change will influence robot's stability and the updated path should be re-planned.

In order to avoid local heading optimal such as caused by VFH, we use a global passable skeleton map which is derived from passable area thinning based on the popular Zhang-Suen algorithm to select optimal connecting point [21]–[23]. The method is shown below.

A binary digital image is defined by matrix $I(i, j)$, where each pixel is either background (obstacle grid) 0 or foreground (free grid) 1. The pixels $P_2, \ldots, P_9$ are the 8- neighbors of the P_1 pixel denoted by $N_8(P_1)$ and labeled as shown in Fig. 6. The thinning process is conducted by applying the following two steps for all the pixels.

In the first sub-iteration, the contour point P_1 is deleted if it satisfies the following conditions:

$$2 \leq B(P_1) \leq 6 \tag{8}$$
$$A(P_1) = 1 \tag{9}$$
$$P_2 * P_4 * P_6 = 0 \tag{10}$$
$$P_4 * P_6 * P_8 = 0 \tag{11}$$

where $A(P_1)$ is the number of 0 to 1 patterns in the ordered set $P_2, P_3, \ldots, P_9$ that are the eight neighbors of P_1, and $B(P_1)$ is the number of nonzero neighbors of P_1, that is,

$$B(P_1) = P_2 + P_3 + P_4 + \cdots + P_8 + P_9 \tag{12}$$

In the second sub-iteration, only conditions (10) and (11) are changed as follows:

$$P_2 * P_4 * P_8 = 0 \tag{13}$$
$$P_2 * P_6 * P_8 = 0 \tag{14}$$

and the rest remain the same. This process is repeated until only the occupied cells belonging to the medial skeleton of the object remain.

The results of thinning process are shown in Fig. 7, we can see that the Zhang-Suen algorithm yields very good results for global connectivity.

But the path start point and end point are not shown on the graph using Zhang-Suen algorithm, thus we do not know

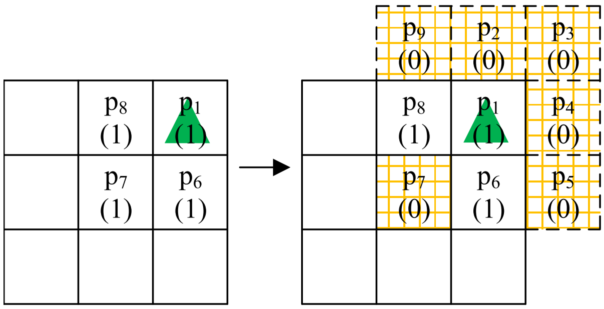

FIGURE 8. Corner grid modification.

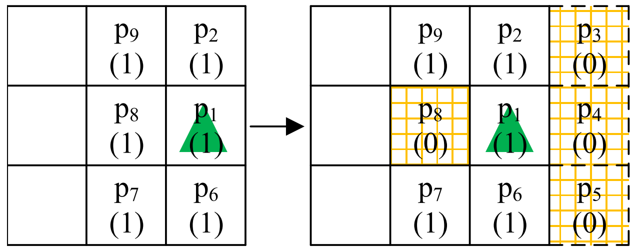

FIGURE 9. Edge grid modification.

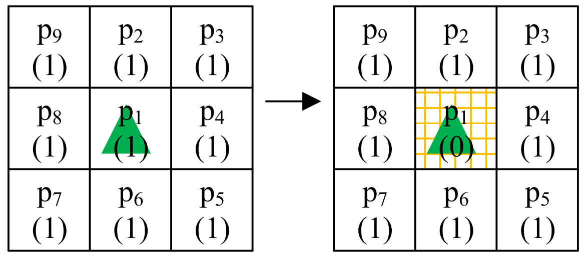

FIGURE 10. Inner grid modification.

if the skeleton would connect with these points. For this reason, it needs further improvement to obtain the skeleton connecting start point and end point. According the principle of Zhang-Suen algorithm, contour point P_1 will be deleted if it satisfies (8), (9), (10), (11) or (8), (9), (13), (14), thus the point will be reserved if we modify the 8-neighbors so as it does not fit above conditions.

Firstly, the start or end point is projected to a grid, denoted by p_1, and set it as free grid as well as its 8 neighboring cells.

$$p_i = i(i = 1, 2, \ldots, 9) \tag{15}$$

If p_1 is a corner grid (top left, top right, bottom left, bottom right) typified by the green triangle shown in the left of Fig. 8, there will be five girds of its 8-neighbors located in the outer section of the map as shown as dotted blocks, treating these as obstacles. Equation (8) and (9) will not be achieve at the same time if the diagonal grid p_7 is reset to 0, so the p_1 will be reserved in this case.

$$p_i = 1 \begin{cases} \text{if } p_1 \text{ is a corner} \\ \& \\ p_i \text{ and } p_1 \text{ are diagonal grids} \end{cases} \tag{16}$$

If p_1 is on the edge of the map (top, bottom, left, right) typified by the green triangle shown in Fig. 9, there will be three girds of its 8-neighbors located in the outer section of the map as shown as dotted blocks, treating these as obstacles. Equation (9) will not be achieve if the inner side grid p_8 is reset to 0, so the p_1 will be reserved in this case.

$$p_i = 0 \begin{cases} \text{if } p_1 \text{ is an edge grid } \& \\ i = 2, 3, 4, \ldots, 9 \;\& \\ p_i \text{ is inner an perndicular to } p_1 \end{cases} \tag{17}$$

Though all equations will not be achieved if p_1 is inside the map as shown in Fig. 10, the 3*3 window will be deleted with iteration or a simply connected skeleton may be reserved. In order to make sure p_1 will connect with the skeleton, according to principle of Zhang-Suen algorithm that if p_1 is a background point and all of its 8 neighboring grids are foreground, the 8-neighbors will be reserved as skeleton. So p_1 will connect with the skeleton by setting it to 0 if it is an inner point.

$$p_1 = 0 \begin{cases} \text{if } p_1 \text{ is an inner grid} \\ \& \\ p_i = 1 \; i = 2, 3, 4, \ldots, 9 \end{cases} \tag{18}$$

Through the above improving measures, the skeleton connecting with the path start point and end point can be obtained as shown in Fig. 11.

For the map shown in Fig. 5(b), there will be four path points (r_1, r_2, r_3, r_4) can be obtained by LOS using walkable skeleton as shown in Fig. 12(a). The desirable direction angle γ_3 passing r_3 which is shown with solid arrow is the closest to the previous angle γ_1. Thus a new route from r_3 to the path start point and end point can be re-planned by A* as showed in Fig. 12(b) and this path will satisfy the heading constraint.

IV. SIMULATION EXPERIMENT

In order to evaluate the performance of AT*, some simulating experiments using Webots robotics simulator are done. The simulation scene is shown in Fig. 13. SICK LMS291 sensor is used to get environmental depth information and identify obstacles. Robots heading angle is measured by a compass sensor. A moving red target can be recognized by the camera and the angle between robot and target also can be worked out with the camera, then LMS291 will get the location of the target at this angle.

Environment information within 5.0m*5.0m is updated in a dynamic rolling window and the map is built with regularly sized grid cells as 10cm*10cm, as shown in Fig. 14. The blue path is planned by AT* and the green is a smoothed path by quadratic B-splines curve. A robot as shown in the blue semicircle will move toward to the red point obtained by LOS.

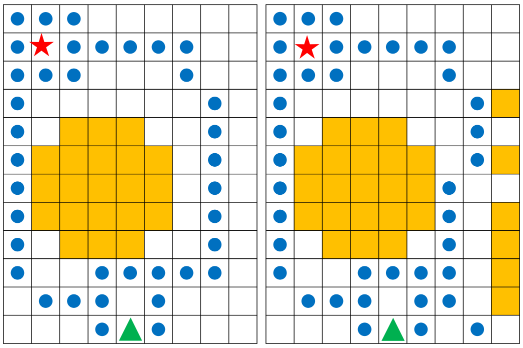

(a) Improved passable skeleton of simple maps

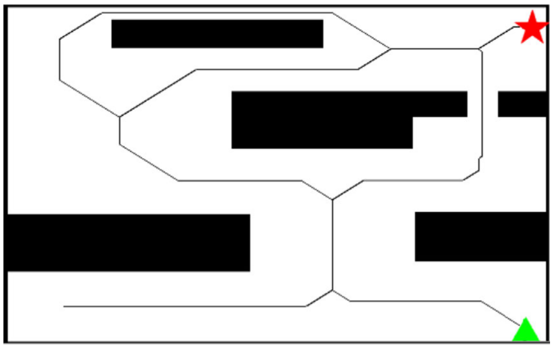

(b) Improved passable skeleton of complicated maps

FIGURE 11. Thinning of different maps with improved algorithm.

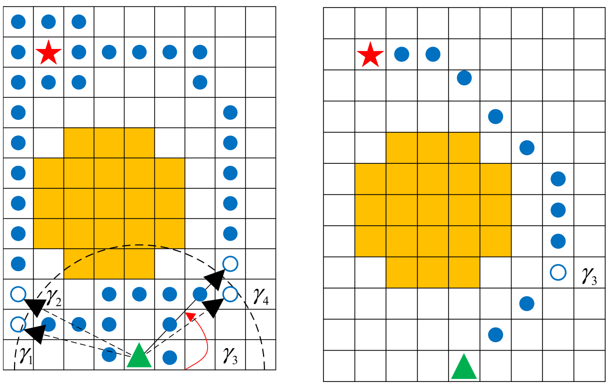

(a) Connecting point selection (b) Re-planned path

FIGURE 12. Selection of connecting point and path re-planning.

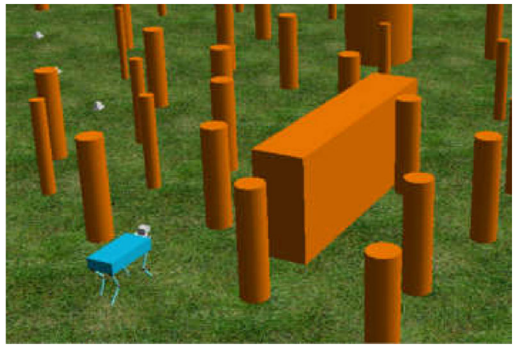

FIGURE 13. Webots simulation scenario.

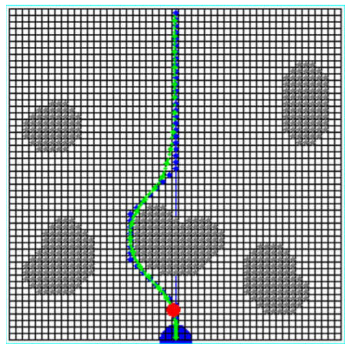

FIGURE 14. Environment representation and path generation.

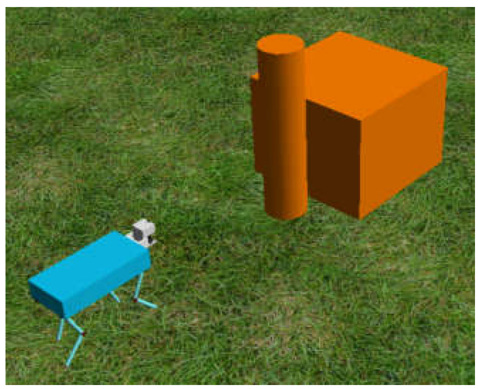

FIGURE 15. Static target following scenario.

Firstly, we teste the difference between A* and AT* in the scenario as shown in Fig. 15. The target is static and in front of the robot with a distance of 6.5m.

A series of obstacle avoidance path planned by A* are shown in Fig. 16. We can see that there are obvious path changes on both side of obstacles by the lack of heading constraints. These changes will adversely affect the safety of robots especially when robots are close to the obstacle.

The following illustration shows a series of obstacle avoidance path planned by AT*. When the difference between desirable heading angle of adjacent time is greater than the threshold, AT* will look for a path point with minor heading fluctuation using walkable skeleton as shown with magenta color, then a path passing this point will be re-planned. The heading will be more successive by this way.

A comparison of the full trajectory and desirable heading angles planned by A* and AT* are shown in Fig. 18. Red asterisks and line segments mean the path point and desirable heading angles planned by A*, and blue is planned by AT*. There is an obvious heading fluctuation shown with an arrow on the path planned by A*.

The above two curves of Fig. 19 show the value of desirable heading angles which are planned by A* and AT* with red and blue asterisks respectively. The bottom two curves show the absolute difference of heading angle at adjacent moment.

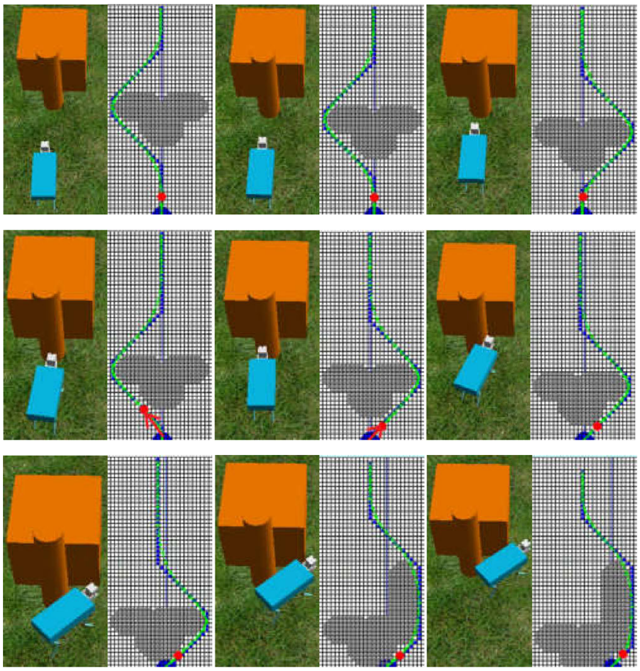

FIGURE 16. Obstacle path planned by A*.

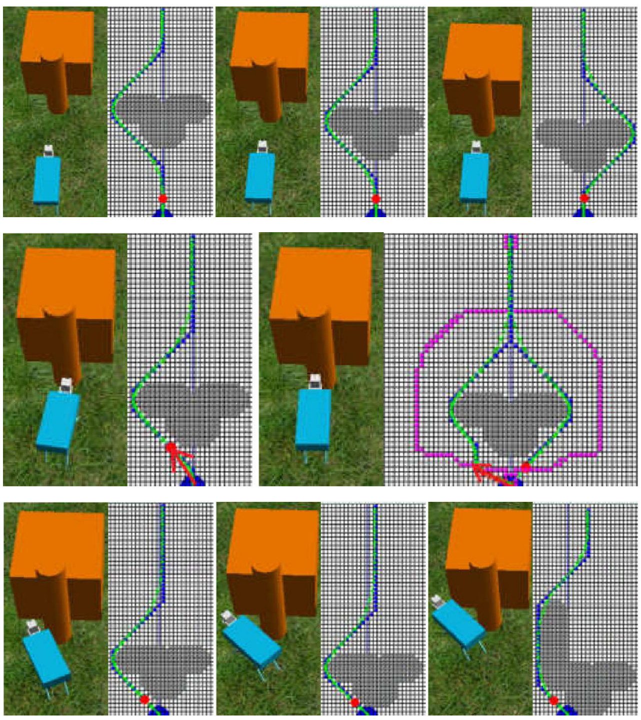

FIGURE 17. Obstacle path planned by AT*.

We can see that the heading change planned by AT* is less than A*

Fig. 20 shows the simulation scenario of moving target following. The red object represents a target and the orange object is an obstacle.

A series of following path near obstacle planned by A* are shown in Fig. 21. There is an obvious heading change as shown by the red arrow which leads to the robot has

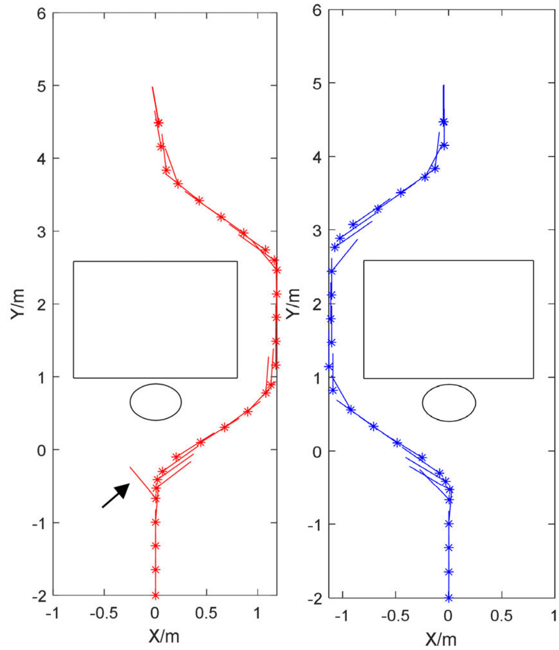

FIGURE 18. The full trajectory of static target following.

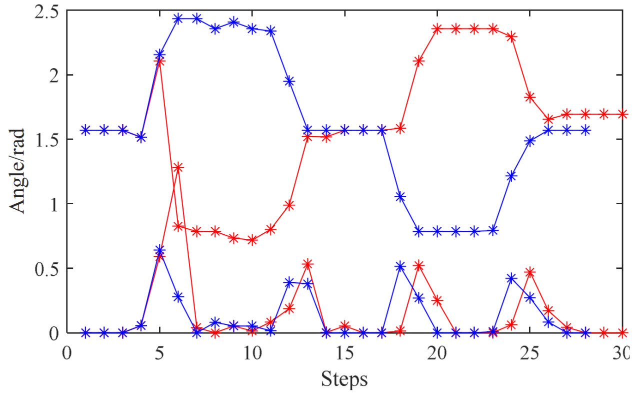

FIGURE 19. The comparison of heading angle.

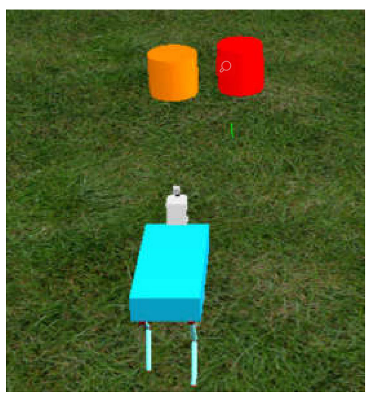

FIGURE 20. Moving target following scenario.

not succeeded in heading adjustment and collide with the obstacle.

Fig. 22 shows a series of following path near the obstacle planned by AT*. There are two times thinning operations when the difference between desirable heading angle

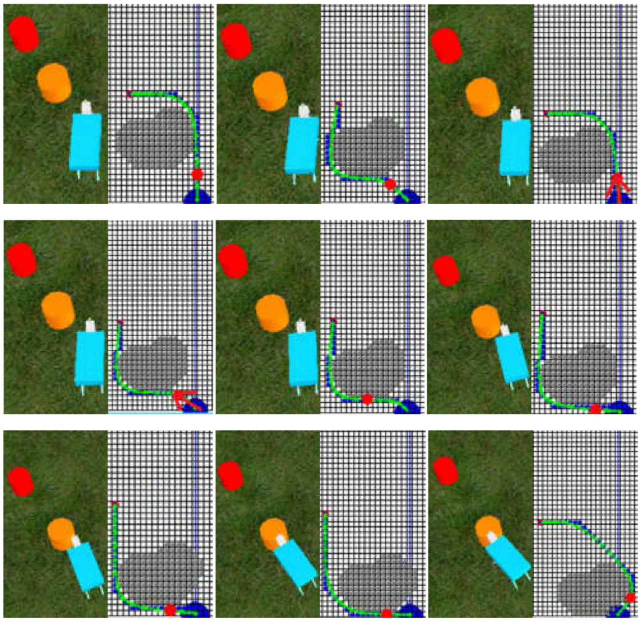

FIGURE 21. Obstacle path planned by A*.

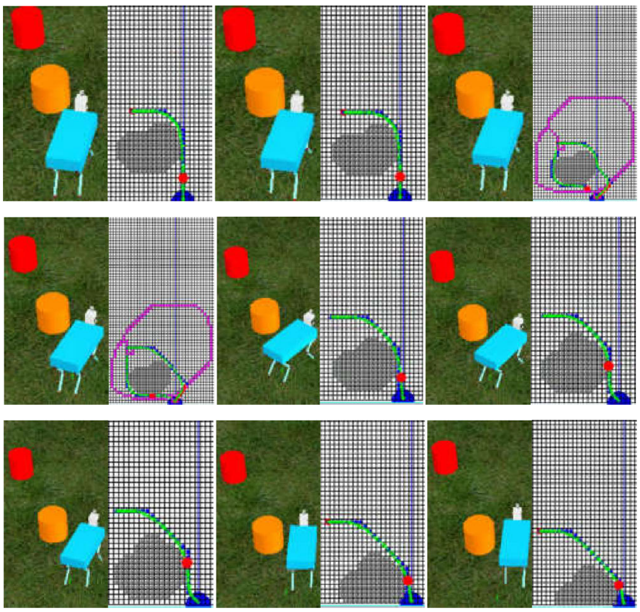

FIGURE 22. Obstacle path planned by AT*.

of adjacent time is greater than the threshold, and the robot can avoid obstacle successfully along the re-planned path.

A comparison of the full moving target tracking trajectory and desirable heading angles planned by A* and AT* are shown in Fig. 23. Green points are the target trajectory. Red asterisks and line segments mean path points and heading angles planned by A*, and blue is planned by AT*. The robot collides with the obstacle along red path due to the fluctuation of desirable heading angle. In contrast, the robot avoids obstacle and follows target successfully along the blue path.

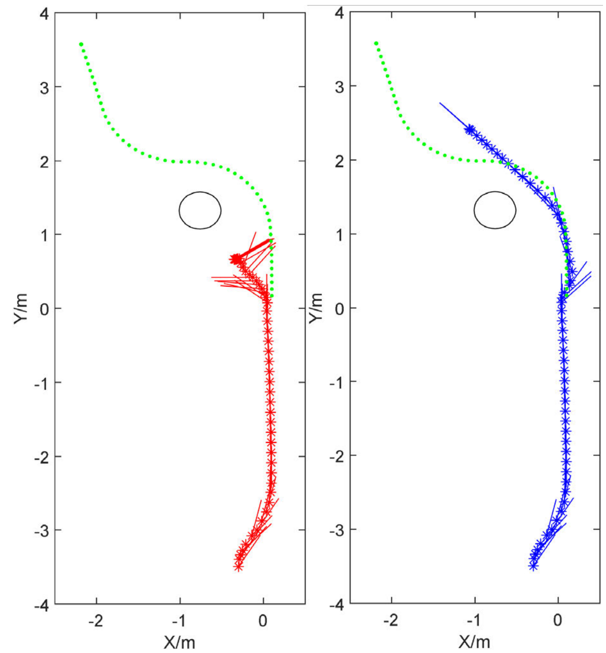

FIGURE 23. The full trajectory of moving target following.

V. CONCLUSION

In dynamic unknown environment, the topic of path planning has always been a challenge for HFRs. They will need to re-plan path timely according the change of obstacles and target position. But the traditional path planning algorithm is generally focused on how to avoid obstacles or connect with the new target position, there are rarely studies on the elimination of robot heading fluctuation which is caused by path re-planning. To address this, a novel dynamic path re-planning method AT* based on A* algorithm and walkable area thinning is proposed. When robots heading difference value between the current and last moment which is derived from the path planned by A* exceeds the threshold, AT* will search for connection points by walkable area thinning, and then a new path going through optimal connection point and meeting heading constraints will be re-planned. Thinning algorithm is improved in order to make the passable skeleton can connect path origin and the end. With these modifications AT* ensures HFRs heading stability in dynamic path re-planning. In the future, we will continue to improve the obstacle avoidance strategies and solve the path planning problem of target missing.

REFERENCES

[1] S. S. Honig, T. Oron-Gilad, H. Zaichyk, V. Sarne-Fleischmann, S. Olatunji, and Y. Edan, "Toward socially aware person-following robots," *IEEE Trans. Cognit. Develop. Syst.*, vol. 10, no. 4, pp. 936–954, Dec. 2018, doi: 10.1109/TCDS.2018.2825641.

[2] H.-M. Gross, K. Debes, E. Einhorn, S. Mueller, A. Scheidig, C. Weinrich, A. Bley, and C. Martin, "Mobile robotic rehabilitation assistant for walking and orientation training of stroke patients: A report on work in progress," in *Proc. IEEE Int. Conf. Syst., Man, Cybern. (SMC)*, San Diego, CA, USA, Oct. 2014, pp. 1880–1887, doi: 10.1109/SMC.2014.6974195.

[3] L. Bodenhagen, S. D. Suvei, W. K. Juel, E. Brander, and N. Krüger, "Robot technology for future welfare: Meeting upcoming societal challenges–an outlook with offset in the development in Scandinavia," *Health Technol.*, vol. 9, no. 3, pp. 197–218, Feb. 2019, doi: 10.1007/s12553-019-00302-x.

[4] L. Yu and K. Zhou, "A dynamic local path planning method for outdoor robot based on characteristics extraction of laser rangefinder and extended support vector machine," *Int. J. Pattern Recognit. Artif. Intell.*, vol. 30, no. 2, 2016, Art. no. 1659004, doi: 10.1142/S0218001416590047.

[5] X. Hu, L. Chen, B. Tang, D. Cao, and H. He, "Dynamic path planning for autonomous driving on various roads with avoidance of static and moving obstacles," *Mech. Syst. Signal Process.*, vol. 100, pp. 482–500, Feb. 2018, doi: 10.1016/j.ymssp.2017.07.019.

[6] N. B. Abdul Latip, R. Omar, and S. K. Debnath, "Optimal path planning using equilateral spaces oriented visibility graph method," *Int. J. Electr. Comput. Eng.*, vol. 7, no. 6, pp. 3046–3051, Dec. 2017, doi: 10.11591/ijece.v7i6.pp3046-3051.

[7] Y. Jiang, C. Yang, Z. Ju, and J. Liu, "Obstacle avoidance of a redundant robot using virtual force field and null space projection," in *Proc. Int. Conf. Intell. Robot. Appl.*, Aug. 2019, pp. 728–739, doi: 10.1007/978-3-030-27526-6_64.

[8] J. S. Kumar and R. Kaleeswari, "Implementation of vector field histogram based obstacle avoidance wheeled robot," in *Proc. Online Int. Conf. Green Eng. Technol. (IC-GET)*, Coimbatore, India, Nov. 2016, pp. 1–6, doi: 10.1109/GET.2016.7916842.

[9] M. R. Jabbarpour, H. Zarrabi, J. J. Jung, and P. Kim, "A green ant-based method for path planning of unmanned ground vehicles," *IEEE Access*, vol. 5, pp. 1820–1832, 2017, doi: 10.1109/ACCESS.2017.2656999.

[10] J. Sun, J. Tang, and S. Lao, "Collision avoidance for cooperative UAVs with optimized artificial potential field algorithm," *IEEE Access*, vol. 5, pp. 18382–18390, 2017, doi: 10.1109/ACCESS.2017.2746752.

[11] H. Zhang, L. Dou, H. Fang, and J. Chen, "Autonomous indoor exploration of mobile robots based on door-guidance and improved dynamic window approach," in *Proc. IEEE Int. Conf. Robot. Biomimetics (ROBIO)*, Guilin, China, Dec. 2009, pp. 408–413, doi: 10.1109/ROBIO.2009.5420681.

[12] X. Liu, Y. Li, J. Zhang, J. Zheng, and C. Yang, "Self-adaptive dynamic obstacle avoidance and path planning for USV under complex maritime environment," *IEEE Access*, vol. 7, pp. 114945–114954, 2019, doi: 10.1109/ACCESS.2019.2935964.

[13] T. Zeng and B. Si, "Mobile robot exploration based on rapidly-exploring random trees and dynamic window approach," in *Proc. 5th Int. Conf. Control, Autom. Robot. (ICCAR)*, Beijing, China, Apr. 2019, pp. 51–57, doi: 10.1109/ICCAR.2019.8813489.

[14] P. Saranrittichai, N. Niparnan, and A. Sudsang, "Robust local obstacle avoidance for mobile robot based on dynamic window approach," in *Proc. 10th Int. Conf. Electr. Eng./Electron., Comput., Telecommun. Inf. Technol.*, Krabi, Thailand, May 2013, pp. 1–4, doi: 10.1109/ECTICon.2013.6559615.

[15] Y. Zhang, Z. Liu, and L. Chang, "A new adaptive artificial potential field and rolling window method for mobile robot path planning," in *Proc. 29th Chin. Control Decis. Conf. (CCDC)*, Chongqing, China, May 2017, pp. 7144–7148, doi: 10.1109/CCDC.2017.7978472.

[16] L. Zhe, L. Yibin, R. Xuewen, and Z. Hui, "Path planning based on ADFA algorithm for quadruped robot," *IEEE Access*, vol. 7, pp. 111095–111101, 2019, doi: 10.1109/ACCESS.2019.2920420.

[17] X. Chen, D. Liu, and T. Tang, "Path planning for UCAV in dynamic and uncertain environments based on focused D algorithm," in *Proc. 4th Int. Symp. Comput. Intell. Design*, Hangzhou, China, Oct. 2011, pp. 55–58, doi: 10.1109/ISCID.2011.115.

[18] Z. Hui, R. Xuewen, L. Yibin, L. Bin, Z. Junwen, and Z. Qin, "Path planning based on sliding window and variant A algorithm for quadruped robot," *High Technol. Lett.*, vol. 22, no. 3, pp. 334–342 Jun. 2016, doi: 10.3772/j.issn.1006-6748.2016.03.013.

[19] D. Wooden, M. Malchano, K. Blankespoor, A. Howardy, A. A. Rizzi, and M. Raibert, "Autonomous navigation for big dog," in *Proc. IEEE Int. Conf. Robot. Autom.*, Anchorage, AK, USA, May 2010, pp. 4736–4741, doi: 10.1109/ROBOT.2010.5509226.

[20] W. Chen, N. Wang, X. Liu, and C. Yang, "VFH based local path planning for mobile robot," in *Proc. 2nd China Symp. Cognit. Comput. Hybrid Intell. (CCHI)*, Xi'an, China, Sep. 2019, pp. 18–23, doi: 10.1109/CCHI.2019.8901916.

[21] K. Xu, R. Fu, L. Deng, Y. Ou, and X. Wu, "A fast robot path planning algorithm based on image thinning," in *Proc. Int. Conf. Intell. Robot. Appl.*, Berlin, Germany, Nov. 2010, pp. 548–557, doi: 10.1007/978-3-642-16584-9_53.

[22] P. Tarabek, "A robust parallel thinning algorithm for pattern recognition," in *Proc. 7th IEEE Int. Symp. Appl. Comput. Intell. Informat. (SACI)*, Timisoara, Romania, May 2012, pp. 75–79, doi: 10.1109/SACI.2012.6249979.

[23] T.-B. Kwon and J.-B. Song, "Thinning-based topological exploration using position possibility of topological nodes," *Adv. Robot.*, vol. 22, nos. 2–3, pp. 339–359, Jan. 2008, doi: 10.1163/156855308X292619.

HUI ZHANG received the bachelor's and master's degrees from Shandong Agricultural University, China, in 2009 and 2012, respectively, and the Ph.D. degree from Shandong University, China, in 2016. He is currently a Lecturer with the School of Electrical Engineering and Automation, Qilu University of Technology (Shandong Academy of Sciences), China. His research interests include the environmental perception and path planning for mobile robots.

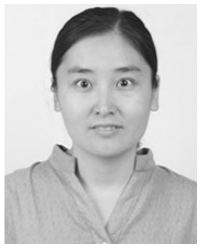

PEI WANG received the Ph.D. degree in control theory and control engineering from Shandong University, in 2016. She is currently a Lecturer with the School of Electrical Engineering and Automation, Qilu University of Technology (Shandong Academy of Sciences), China. Her research interest includes the control and applications of fractal.

YOUPAN ZHANG is currently pursuing the bachelor's degree with the School of Electrical Engineering and Automation, Qilu University of Technology (Shandong Academy of Sciences), and has a second-author conference publication. His research interests include path planning, and he has a deep interest in image recognition.

BIN LI received the bachelor's, master's, and Ph.D. degrees in control science, operational research and cybernetics, and pattern recognition and intelligent system from Shandong University, China, in 2002, 2005, and 2012, respectively. He is currently an Associate Professor with the School of Science, Qilu University of Technology (Shandong Academy of Sciences), China, and holds a postdoctoral position at Shandong University. His research interests include algorithms for neural networks, gait planning, and adaptive control of legged robots.

YONGGUO ZHAO received the bachelor's, master's, and Ph.D. degrees from Shandong University, China, in 2001, 2004, and 2008, respectively. He is currently the Associate Director of the Institute of Automation, Qilu University of Technology (Shandong Academy of Sciences). He has taken charge of five state or province projects such as National International Science and Technology Cooperation Project, Major Scientific and Technological Innovation Projects in Shandong Province, and Science and Technology Research Project of Shandong Province. His research interests include robotics, intelligent manufacturing equipment, and automated production lines.